Rapid Detection of *Staphylococcus aureus* Using Paper-Derived Electrochemical Biosensors

Lucas de Brito Ayres[a], Jordan Brooks[a], Kristi Whitehead[b], and Carlos D. Garcia[a*]

[a]Department of Chemistry and [b]Department of Biological Sciences

Clemson University, Clemson, South Carolina, 29634, USA

[*] To whom correspondence should be addressed: cdgarci@clemson.edu

ABSTRACT

Several groups have recently explored the idea of developing electrochemical paper-based wearable devices, specifically targeting metabolites in sweat. While these sensors have the potential to provide a breath of analytical information, there are several key challenges to address before these sensors can be widely adopted for clinical interventions. Towards this goal, this report describes the development of a paper-based electrochemical sensor for the detection of *S. aureus*. Enabling the application, this report describes the fabrication of paper-derived carbon electrodes, which were modified with a thin layer of sputtered gold (that minimizes lateral resistivity and significantly improves the electron transfer process) and with chitosan (used as a binder to offer flexibility). The resulting material was laser-patterned and applied for the development of an electrochemical biosensor controlled (via a wireless connection) by a custom-built, portable potentiostat. As no interference was observed when exposed to other bacteria or common metabolites, this wearable system (paper-derived electrodes + potentiostat) has the potential to detect the presence of *S. aureus* in skin, a commonly misdiagnosed and mistreated infection.

KEYWORDS:

Wearable, paper-based analytical device, portable potentiostat, *Staphylococcus aureus*.

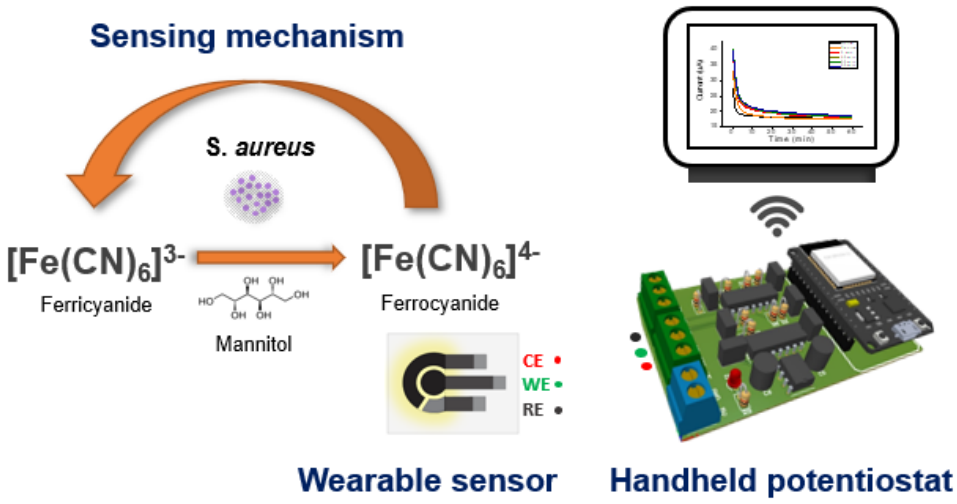
Sensing mechanism
S. aureus
[Fe(CN)6]3-
Ferricyanide
Mannitol
[Fe(CN)6]4-
Ferrocyanide
CE
WE
RE
Wearable sensor
Handheld potentiostat

1. INTRODUCTION

Paper-based analytical devices (μPADs)[1] and their electroanalytical derivations (ePADs)[2] play an important role as modern analytical tools and have been applied in several areas such as medicine,[3-5] forensics,[6, 7] food science,[8, 9] environmental analysis,[10] and the pharmaceutical industry.[11] When deployed as point-of-care (POC) sensors, these devices can provide appropriate sensitivity to detect not only metabolites but also pathogens such as SARS-CoV-2,[12] ebola,[13] *Escherichia coli* (*E. coli*),[14] or *Staphylococcus aureus* (*S. aureus*).[15, 16] Considering that paper represents one of the most appealing materials to be attached to skin (inert, low-cost, non-toxic, and flexible), several groups have recently explored the idea of developing paper-based wearable devices, specifically targeting metabolites in sweat.[17, 18] In general, these sensors can not only play an essential role as a non-invasive tools to monitor multiple analytes in real time[19-21] but also provide information complementary to that potentially obtained by more complex (and invasive) systems.[5, 22-24] In addition, and while these sensors have the potential to diversify the substrates available for wearable devices, one key challenge is to ensure that the analytical performance of these sensors is not significantly affected during use (bending, movement, etc.)[25, 26] and over multiple detection cycles. This is especially true for sensors based on electrochemical methods, that typically rely on a relatively narrow selection of electrode materials.[27] In fact, most reported ePADs targeting the detection of pathogens are based on conductive carbon-based materials (e.g., nanotubes, carbon fibers, or graphene)[28-30] placed on a polymeric substrate and coated with metallic nanoparticles[31-34] and/or biomolecules (e.g. aptamers, enzymes, or antibodies).[35-37] Albeit functional, these sensors are typically expensive, offer limited options in terms of functional design, and require complex instrumentation for their manufacturing;[38] thus limiting the deployment and widespread implementation of wearable ePADs for POC applications.

Aiming to extend the applicability of ePADs, our group reported the possibility to implement pyrolyzed paper as an active substrate for the development of detection electrodes.[39, 40] This material is produced via a simple manufacturing process and features competitive electrochemical activity, low cost, and the possibility to implement a wide variety of functionalization protocols. Nevertheless, and despite those advantages, pyrolyzed paper has not been explored as active material for developing wearable devices,

probably due it its brittleness and the challenges associated with its resistivity, which often limits its application to low-frequency methods (such as amperometry).

Addressing these limitations, we herein report the modification of this material with a thin layer of sputtered gold (that minimizes lateral resistivity and significantly improves the electron transfer process) and with chitosan (used as a binder and offering flexibility). The resulting material was laser-patterned and applied for the development of a paper-based electrochemical biosensor for the detection of bacteria. The biosensor was controlled using a custom-built potentiostat (via a wireless connection) and applied to detect the presence of *S. aureus* via the oxidation of the ferrocyanide (produced by the bacteria's respiration cycle) in the presence of mannitol. It is worth mentioning that while other electroanalytical strategies have been reported to perform antibiotic susceptibility tests for *E. coli*,[41-44] the proposed approach represents the first use of a low-cost, electrochemical biosensor fabricated from paper and used to detect *S. aureus*. Considering that the proposed approach does not rely on the use of protein-based recognition elements (used in traditional colorimetric[45-47] or electrochemical sensors[48-50]), we believe this work has the potential to address a clinical need to identify the presence of *S. aureus* in skin, a commonly misdiagnosed and mistreated infection.[51-53] Moreover, the presented potentiostat would not only allow full mobility of the patient but also the collection of the results in a wide variety of web-based platforms.

2. MATERIAL AND METHODS

2.1. Electrode Fabrication. Electrodes were obtained by pyrolysis of paper (Whatman 3MM chromatography paper; GE Health Care; Pittsburgh, PA) using a tube furnace (Type F21100, Barnstead–Thermolyne; Dubuque, IA, USA) and following a previously reported procedure.[30–32] Next, the pyrolyzed samples were removed from the furnace and gold sputtered (35 $\mu g/cm^2$, 108 Auto sputter coater; Cressington Scientific Instruments, UK). Then, the electrodes were cut using a commercial 30W CO_2 laser engraver (Mini24, Epilog Laser Systems; Golden, CO, USA) and respective areas of the device were painted with Ag/AgCl ink (CI-4025, Engineered Materials Systems; Delaware, OH) to define the reference electrode or silver paint (SPI Supplies; West Chester, PA, USA) to facilitate the electrical contact with the potentiostat. In order to provide a robust connection with the potentiostat, a small piece of aluminum tape

was applied to the tip of the electrodes, allowing the (temporary) use of alligator clips without breaking the carbon layer. Next, chitosan was applied to the electrodes (to provide structural stability to the carbon fibers) by evenly spreading 40 μL of a solution containing the polymer on the electrodes and allowing it to dry in a convection oven at 65 °C for 1 hour. To prevent water from wicking up the stem of the electrodes (and therefore increasing the electrode area), a layer of silicone was applied to cover the connections and leave the detection electrodes unexposed. Finally, the ensemble was pressed in a thermal press (100 °C) for 10 min and then stripped 20-gauge tinned copper wires were attached to the stem of the electrodes. Figure 1 provides a schematic summary of the process as well as the shape and disposition of the electrodes.

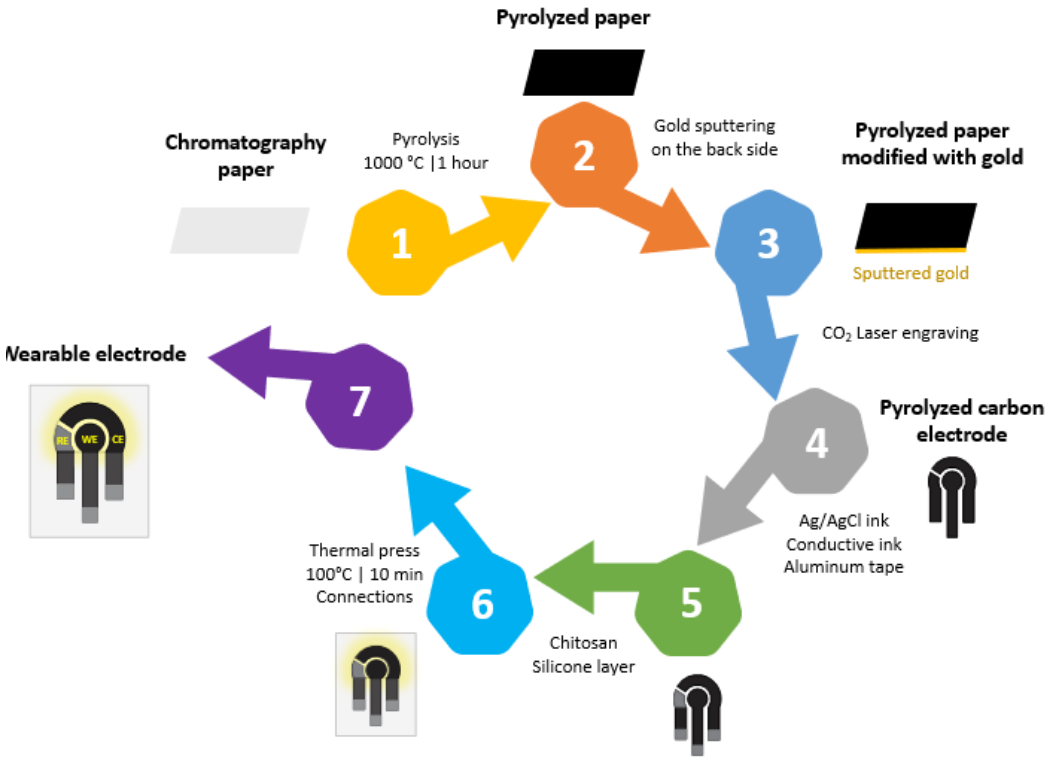

Figure 1: Schematic summary of the process used to fabricate the electrodes used for the wearable device.

2.2. Solutions and reagents. Details regarding the preparation of solutions, including the procedures for bacterial growth are provided as Supplementary Information.

2.3. Sensing mechanism. A wide number of sensors and biosensors for pathogen detection have been reported, based on either antibodies or enzymatic activity.[49, 54, 55] In addition to those, respirometric assays (those based on monitoring the microbial reduction rate of an electron acceptor (e.g. oxygen, nitrate,

ferricyanide, benzoquinone, etc.)[56] are particularly useful because they provide information related to the microbial metabolic activity. More importantly, since these sensors are not using protein-based biorecognition elements, have the potential to enable the development of sensors with much longer shelf-life. Several groups have reported the capacity of various bacteria to reduce $K_3Fe[CN]_6$,[41-44, 57] signal that not only provides information about the concentration of viable cells in the culture but can also reach limits of detection as low as 1 CFU/mL.[54] Towards this goal, the experiments herein described were performed following the oxidation of $K_4Fe[CN]_6$ (at 0.4V, *vide infra* Figure 5A), produced by the bacteria from $K_3Fe[CN]_6$ in the presence of mannitol, which serves as differential agent for the identification of *S. aureus* from various samples.[58, 59]

2.4. Potentiostat. To enable the use of the proposed ePAD as a wearable device, a custom potentiostat capable of performing CV and (if required) amperometry was developed. Specific details for the design, including parts, are provided as Supplementary Information. Briefly, a new circuit layout was developed to integrate a microcontroller (built-in Wi-Fi and Bluetooth, 12 bits ADC and 8 bits DAC) an operational amplifier and a 5000mAh / 5V rechargeable battery. The instrument was controlled using a GUI compatible with web browsers as well as the Internet of Things (IoT) protocols.

3. RESULTS AND DISCUSSION

The goal of the following section is to investigate the electrochemical performance of the proposed device throughout the optimization steps as well as the use of the proposed sensor in combination with the developed portable potentiostat as a POC sensing platform to detect *S. aureus*. Additional information related to the analytical instrument (e.g., firmware, electronic, and printed circuit board) as well as additional results for calibration and validation of the instrumentation are presented in the Supplementary Material of this manuscript.

3.1. Effect of the sputtered gold film. The addition of a metallic layer on the back side of the electrodes intends to decrease the lateral resistivity between the electrical contact and the detection area of the electrode. While this aspect plays a critical role when those electrodes are applied in high-frequency

electroanalytical techniques (e.g., electrochemical impedance spectroscopy or differential pulse voltammetry),[60] the overall resistivity of the substrate may also impact the analytical performance of the sensor when other techniques (such as CV) are used. While several authors have described the use of gold leaf as an inexpensive material towards the fabrication of electrodes,[61-63] we selected vapor deposition considering the increased practicality, reproducibility, and speed of the method. It is important to mention that for these experiments, only a small amount of gold (35 $\mu g/cm^2$) was required to significantly decrease the lateral resistance of the paper-derived carbon electrodes (< 1Ω, from the contact point to the middle of the detection spot, see Figure 1). The effectiveness of this strategy was assessed by CV (at various scan rates), considering both the peak current and the peak potential obtained with a solution containing 5 mM ferrocyanide and PBS (pH 7.4). Representative results of these experiments are summarized in Figure 2.

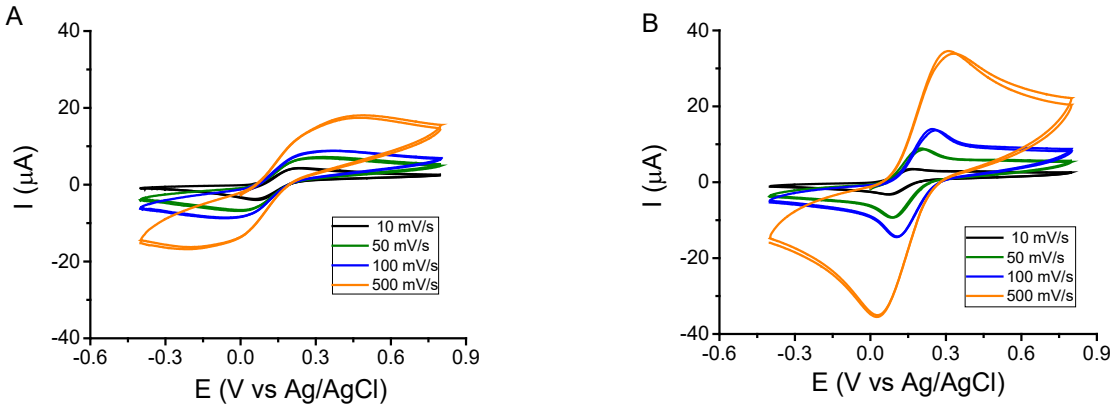

Figure 2: Cyclic voltammograms obtained using ferrocyanide (5 mM in PBS) at various scan rates recorded by using the bare paper-derived sensor (A) or modified with a layer of gold in the back side (B).

As it can be observed in Figure 2A, results obtained with the plain paper-derived carbon electrodes feature one clear anodic peak and the corresponding cathodic peak, where significant shifts in peak potential and distortions in both anodic and cathodic peaks are noted, as the sweep rates increases. This behavior, that is also observed when the signal is affected by uncompensated ohmic drop,[64] was attributed to the lateral resistance of the material; issue that becomes dominant where the change in the signal imposed is faster than the electron transfer process and that has been reported for many other (resistive) materials.[65-68] On the contrary, and while the response is far from reversible (requiring ΔEp = 59 mV), the incorporation of the layer of gold led to significant improvements in the electrochemical reaction (ΔEp between 83 mV and 278 mV, Figure 2B) with respect to the bare electrode. Additionally, it is important to note that the peak current

obtained at 500 $mV.s^{-1}$ with the gold-modified electrode is substantially larger (approximately twice as large) than that of the commercial glassy carbon electrode (both displaying the same geometrical area, 0.125 cm^2, Figure SI 2) at the same scan rates. This enhanced performance can be attributed to the increased surface area and 3D morphology of the paper-derived electrodes, as previously reported by our group.[40, 60] The inter-electrode reproducibility (pyrolyzed electrodes derived from different paper sheets) was measured by cyclic voltammetry using 5 mM ferro/ferricyanide, rendering a relative standard deviation for the anodic peak was ±5.6% (n=5), which was considered acceptable for the scope of the project.

It is also worth mentioning that at low sweep rate (10 - 50 $mV.s^{-1}$), the anodic peak current for the bare paper-derived electrode (Ip_a = 4.2 µA) is only slightly larger than the peak current obtained with the gold-modified electrode (Ip_a = 3.4 µA) or the current obtained with the GCE (Ip_a = 3.3 µA). These results are important because they support the notion that the metal sputtered on the backside of the proposed sensor (also shown in Figure SI 2) is not in direct contact with the electroactive species and only improving the electrical properties of the material. Likewise, sputtering a sample of non-pyrolyzed cellulose (under identical conditions) did not render the paper conductive (data not shown), experiment that was performed to demonstrate that the gold layer is only bridging the carbon fibers and not completely covering the bottom of the device. Thus, this simple strategy was implemented to improve the electrochemical response of our paper-derived electrodes and used for all the remaining experiments.

3.2. Effect of the Addition of Chitosan on the Electrochemical Response. Although one of the limitations of the paper-derived electrodes is their brittleness, several authors have reported that chitosan could be used as a binder[69, 70] and potentially applied to mitigate this problem. Thus, the electrochemical behavior of the paper-derived sensors modified with chitosan (40 µL, 0.5%, 1.0%, and 2.0%) was first assessed by cyclic voltammetry (5mM ferrocyanide in PBS buffer, pH 7.4 at several scan rates, and in the -0.2V to +0.6V range). While the results from these experiments (voltammograms featuring a single anodic and a single cathodic peak) are provided as Figure SI 3, two aspects are worth discussing from them. In the first place and as specifically described for the electrode modified with the solution containing 2.0% chitosan (Figure SI 4), linear dependences between the peak current and the square root of the scan rate

were obtained for all the electrodes, suggesting that the rate of electron transfer was diffusion controlled.[71] In addition, all voltammograms showed a significant dependence of the peak potential difference with respect to the sweep rate, that ranged from 80mV to 200mV and that was attributed to due to resistive nature of the material[40, 60, 72, 73] (even after the addition of the gold layer). The second aspect that is important to highlight from these voltammograms is that the addition of chitosan also had a positive effect on the peak current (see Figure SI 5). This behavior has been attributed to enhancements in the electron transfer process due to the favorable electrostatic interactions between the (negatively charged) electroactive species and the (positively charged) surface of the electrode, that is now coated with amino groups from the chitosan layer.[74-76] To further investigate the electrochemical behavior of the electrodes modified with chitosan, electrochemical impedance spectra were obtained in the presence of 5mM ferrocyanide in PBS buffer at 0.15V (half-wave potential), and in the frequency range of 0.01Hz and 10^5 Hz. In line with the results obtained by CV, the Nyquist plots obtained with the described sensors show a clear trend in the response, where the diameter of the semicircle decreases with increasing concentrations of chitosan (Figure SI 6).

To obtain quantitative information related to the electrochemical response, the spectra were fit with a Randles-type equivalent circuit considering the resistance of the solution (R_{SOL}), the capacitance (C_{ELE}) and overall resistance (R_{ELE}) of the electrode, and the interfacial behavior represented by the capacitance of the double layer (C_{DL}) and the charge-transfer resistance (R_{CT}) of the interface. Furthermore, a Warburg impedance (Z_W) was included to account for the diffusion of electroactive species involved in the redox reaction. As a summary, Figure 3A shows the dependance of the charge transfer resistance (R_{CT}) with respect to the concentration of chitosan used to modify the electrodes. As it can be observed, a significant decrease in the R_{CT} was obtained as the chitosan concentration increased, reaching a plateau at 2% (105 ± 3 Ω) and providing a significant improvement with respect to the unmodified electrode system (853 ± 50 Ω). Considering these results, the solution containing 2% chitosan was considered the most suitable one to modify the paper-derived carbon electrodes and used for all remaining experiments.

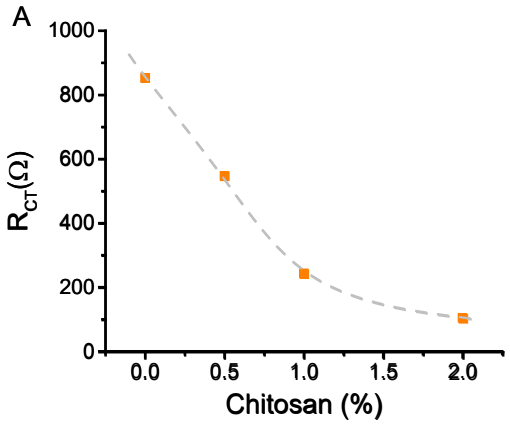

Figure 3A: Dependence of the charge transfer resistance (R_{ct}) as function of the concentration chitosan, added to the paper-derived carbon electrodes. Conditions: 5mM ferri/ferrocyanide in PBS; spectra collected at half-wave potential (0.15V), in the 0.01Hz - 10^5 Hz frequency range and using a 5 mV amplitude.

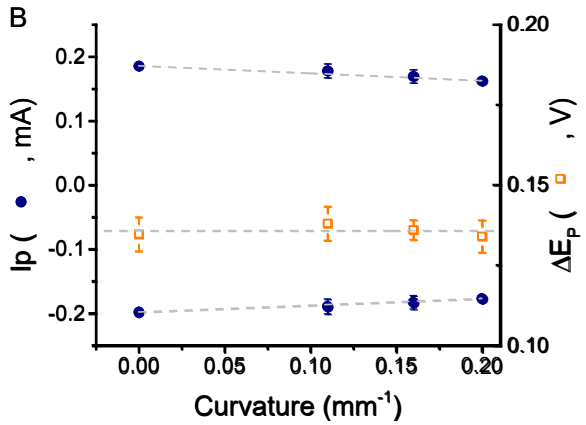

Figure 3B: Influence of the electrode curvature on the peak current (Ip) and peak potential difference (ΔEp) for the proposed paper-derived electrodes modified with 2.0% chitosan. Conditions: 5mM ferri/ferrocyanide in PBS, CV performed in the -0.2V to +0.6V range at 50mV.s^{-1}.

At the core of these experiments involving the addition of chitosan is the need to address the brittleness of the paper-derived electrodes, which would impair their use towards wearable devices as they would otherwise crack as soon as they are attached to skin. Thus, the response of the electrodes modified with the solution containing 2% chitosan was investigated under different curvatures, spanning common body curvatures. These experiments were carried out by attaching the as-prepared electrodes to either a flat surface or various cylindrical objects (with diameters of 5.00 mm, 6.25 mm, or 9.10 mm) and performing cyclic voltammetry (5mM ferri/ferrocyanide in PBS at 50 mV.s^{-1}). The voltammograms are presented in Figure SI 7, and a summary of the corresponding peak currents and peak potential differences are shown in Figure 3B. It can be observed that the electrochemical performance of the curved sensors displays only slight changes with compared to their flat control. As a point of reference, the diameter of children's fingers ranges from 13 mm to 16 mm,[77] supporting the potential use of the proposed electrodes towards the development of wearable devices. While experiments to determine the stability of the material after repeated bending cycles were considered to be outside the scope of this project, our results indicate that the proposed material could be attached to any surface of the body without inducing significant differences due to curvature.

3.3. Portable potentiostat. To enable the potential detection of *S. aureus* infections in skin using the proposed paper-derived electrodes, a portable and Wi-Fi-controlled potentiostat was developed. The electronics of the proposed device are based on the potentiostat described by Meloni,[78] with significant improvements regarding the symmetrical power supply system (ICL7660 and rechargeable LiPo batteries), microcontroller (ESP 32 built-in with Wi-Fi and Bluetooth), and auxiliary filters (described in the circuit diagram, Figure SI 1). As a result, those modifications allowed the miniaturization of the portable instrument to a size that roughly matches a credit card (Figure 4A), in addition to the possibility of using two independent analog-to-digital converters (ADC's) with higher resolution (12 BITS) than similar instruments based on 8 or 10 BITS ADC's.[79, 80] It is also important to mention that although potentiostats with even higher capabilities have been described,[24] the proposed circuitry represents a reasonable balance between performance and cost (<$15, including the battery). The performance of the developed potentiostat was compared against a commercial potentiostat (CHI 660) using three different experiments: I) polarization curve, II) cyclic voltammetry, and III) amperometry. For the first case, the input current for the portable potentiostat was found to behave according to Ohm's law, in addition to matching the current registered using the commercial instrument (Figure SI 9) and suggesting appropriate potential control over the test cell as well as proper instrument calibration. Regarding the CV experiments, well-defined peaks were obtained at the typical potential for the oxidation and reduction process of the studied model couple (ferrocyanide, Figure SI 9), displaying a linear dependence of peak currents in function of the square root of the sweep rate. Finally, amperometric experiments performed with different concentrations of ferrocyanide (5 μM to 5 mM) diluted in PBS buffer were carried out at +0.4V by using the developed potentiostat and compared to those obtained with the commercial instrument (Figure SI 10). As it can be observed in Figure 4B, a good agreement was obtained for the signals collected with both instruments. The sensitivity of the assay was 1.815 ± 0.005 $\mu A.mM^{-1}$_and the limit of detection, calculated as 3.3x σ/S was 8.6 μM (as determined with the commercial potentiostat). It is also important to note that although the portable instrument was only capable of interrogating solutions containing ≥0.1 mM $K_4Fe(CN)_6$ (output currents 0.1 - 10 μA, with current circuitry setup), this range was considered adequate for the intended application.

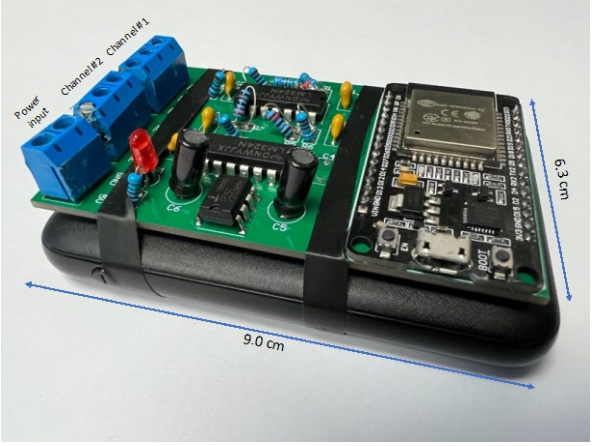

Figure 4A: Picture of the developed portable potentiostat. Dimensions: 9 cm x 6.3 cm x 2.6 cm.

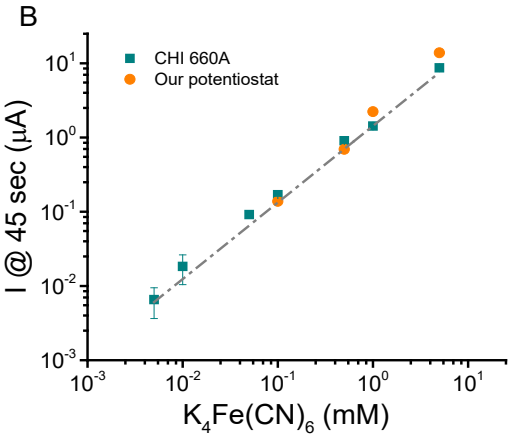

Figure 4B: Currents registered at 45 seconds by both instruments during amperometric experiments of ferrocyanide. Conditions: PBS (pH= 7.4), and fixed applied potential at +0.4V.

3.4. Detection of *S. aureus*. As previously stated, the proposed paper-derived electrodes (modified with the gold layer and chitosan) were used to identify the presence of the pathogen via the electrochemical oxidation of $K_4Fe[CN]_6$, produced by the bacteria in the presence of mannitol. Towards this goal, the effect of the detection potential on the current magnitude was first investigated to ensure an adequate balance between selectivity and sensitivity. Therefore, the electrochemical response of 5mM $K_4Fe(CN)_6$ in PBS pH 7.4 was assessed by performing *I-t* curves (during 180 sec) and covering a potential range from 0.0V to +0.8V. The dependence of the current (measured at 45 sec) and the applied potential is shown in Figure 5A (raw data provided in Figure SI 5). The detection time was selected considering that at that time, stable values in the current were obtained, which not only decreases reading errors but also represents a reasonable analysis time. As it can be observed, a linear increase in the oxidation current of $K_4Fe(CN)_6$ was obtained in the +0.1V to +0.3V, reaching a plateau at approximately +0.4V. This value not only provides the highest sensitivity for the proposed analysis but also avoids the interfering effect from other molecules (salts, glucose, metabolites; data not shown) potentially present in skin.[81, 82] Hence, +0.4V (vs. Ag/AgCl) was chosen as a detection potential and used for all further amperometric experiments.

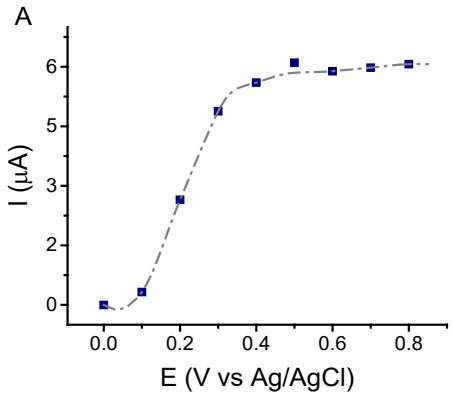

Figure 5A: Cathodic current of 5mM $K_4Fe[CN]_6$ diluted in PBS as a function of the applied potential and measured at 45 sec.

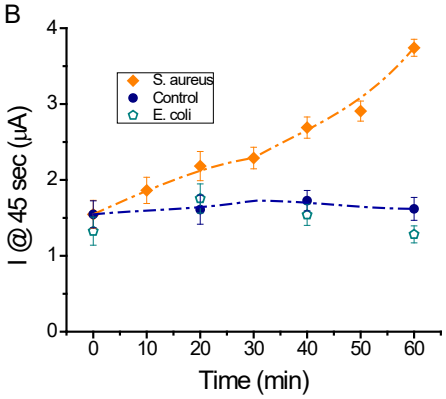

Figure 5B: Current developed as a function of time with a control device (no bacteria), a device containing *S. aureus,* or a device containing *E. coli*. Conditions: 2.5 mM $K_4Fe[CN]_6$ diluted in PBS, detection potential: +0.4V, each measured at 45 sec.

In order to demonstrate the feasibility of the proposed strategy, 50μL of a solution containing approximately 10^4 colonies of *S. aureus* suspended in 1.0 mL of PBS (containing 2.5mM mannitol and 2.5mM $K_3Fe(CN)_6$) were dispensed on the active area of the wearable device and periodically interrogated using amperometry (at +0.4V for 60 sec.) using the portable potentiostat we developed. Moreover, the same experimental conditions were used to run a control device (no added bacteria) or a device seeded with *E. coli*. Those experiments were repeated every 10-20 minutes for 1 hour and Figure 5B shows a summary of the results obtained. As expected, only when the pathogen (*S. aureus*) was metabolically active, a signal evolution was observed. No significant conversion of ferricyanide to ferrocyanide was observed in the control devices (no bacteria) nor the device exposed to *E. coli*, enabling the detection of the pathogen in just 20 min. These results are supported by the capacity of *S. aureus* to preferentially ferment mannitol (over other sugars such as glucose, fructose, or mannose) due to the presence of a phosphotransferase system in the cell wall of this bacteria.[83-85] It is, however, worth mentioning that an initial increase in the oxidation current (only for the initial 20 min) was observed for the device exposed to *E. coli*, results that were attributed to the metabolic activity of the bacteria consuming the remaining nutrients from the original growth media. Additional experiments performed using serial dilutions of the suspension (ranging from 0.1 to 10^3 CFU/mL) also rendered increases in the oxidation current but lower concentrations of bacteria required longer analysis times to develop a measurable signal. Specifically, and although the proposed approach would enable identifying an infection (yes/no answer) within 20 min, the assay can be followed for longer periods

of time (additional 40 min) to render a signal that is proportional to the initial density of bacteria (Figure SI 11) and that can detect down to 0.1 CFU/mL. While a number of technologies have been already presented for the detection of S. aureus,[86-89] including sensors based on aptamers,[90-92] immunoglobulins,[93, 94] proteases,[49] or PCR amplification,[95] the proposed sensor could not only avoid the use of biorecognition elements but also sample pretreatments, as it could be directly applied to the skin.

4. CONCLUSIONS

This work describes a rapid, non-invasive, and low-cost alternative to electrochemically detect *S. aureus* using a paper-derived electrodes and a portable potentiostat. The proposed sensor was derived from pyrolyzed paper and modified by the addition of a thin gold layer (35 $\mu g/cm^2$, in the back side of the electrode) and chitosan. These modifications address the limited resistivity and brittleness of paper-derived electrodes, fundamental limitations common to many carbon-materials. As a result, the electrodes can be deployed as a wearable device, with enhanced performance (lower charge transfer resistance) as well as a response that is independent of the curvatures of the sensor. The combined use of this wearable sensor with the instrument was also demonstrated by detecting the presence of *S. aureus* under optimized experimental conditions, in 20 minutes, and without relying on protein-based biorecognition elements. We believe this is a promising avenue for the implementing of paper-derived electrodes towards a wide variety of point-of-care platforms to monitor skin infections, especially in low-income settings.

5. CONFLICT OF INTEREST

There are no conflicts to declare

6. ACKNOWLEDGMENTS

Authors would like to thank the financial support provided by Clemson University and NASA, via STTR-21-1-T6.06-1513. Jordan Brooks also thanks the support from the REU program at the Department of Chemistry (NSF – Division of Chemistry, award CHE-2050042).

7. REFERENCES

1. Noviana, E.; Ozer, T.; Carrell, C. S.; Link, J. S.; McMahon, C.; Jang, I.; Henry, C. S. Microfluidic Paper-Based Analytical Devices: From Design to Applications. *Chem. Rev.* **2021**, *121*, 11835-11885.

2. Ataide, V. N.; Mendes, L. F.; Gama, L. I. L. M.; de Araujo, W. R.; Paixão, T. R. L. C. Electrochemical paper-based analytical devices: ten years of development. *Anal. Methods* **2020**, *12*, 1030-1054.

3. Mejía-Salazar, J. R.; Rodrigues Cruz, K.; Materón Vásques, E. M.; Novais de Oliveira, O., Jr. Microfluidic Point-of-Care Devices: New Trends and Future Prospects for eHealth Diagnostics. *Sensors* **2020**, *20*.

4. Pillai, S.; Upadhyay, A.; Sayson, D.; Nguyen, B. H.; Tran, S. D. Advances in Medical Wearable Biosensors: Design, Fabrication and Materials Strategies in Healthcare Monitoring. *Molecules* **2021**, *27*.

5. Ye, S.; Feng, S.; Huang, L.; Bian, S. Recent Progress in Wearable Biosensors: From Healthcare Monitoring to Sports Analytics. *Biosensors (Basel)* **2020**, *10*.

6. Ansari, N.; Trambadiya, N.; Lodha, A.; Menon, S. K. A portable microfluidic paper-based analytical device for blood detection and typing assay. *Aust J Forensic Sci* **2021**, *53*, 407-418.

7. de Araujo, W. R.; Cardoso, T. M. G.; da Rocha, R. G.; Santana, M. H. P.; Muñoz, R. A. A.; Richter, E. M.; Paixão, T. R. L. C.; Coltro, W. K. T. Portable analytical platforms for forensic chemistry: A review. *Anal. Chim. Acta* **2018**, *1034*, 1-21.

8. Nilghaz, A.; Mousavi, S. M.; Li, M.; Tian, J.; Cao, R.; Wang, X. Paper-based microfluidics for food safety and quality analysis. *Trends Food Sci Technol* **2021**, *118*, 273-284.

9. Vidal, E.; Domini, C. E.; Whitehead, D. C.; Garcia, C. D. From glow-sticks to sensors: single-electrode electrochemical detection for paper-based devices. *Sens. Diagn.* **2022**, *1*, 496-503.

10. Marquez, S.; Liu, J.; Morales-Narváez, E. Paper-based analytical devices in environmental applications and their integration with portable technologies. *Curr Opin Environ Sci Health* **2019**, *10*.

11. Taghizadeh-Behbahani, M.; Shamsipur, M.; Hemmateenejad, B. Detection and discrimination of antibiotics in food samples using a microfluidic paper-based optical tongue. *Talanta* **2022**, *241*, 123242.

12. Ozer, T.; Henry, C. S. Paper-based analytical devices for virus detection: Recent strategies for current and future pandemics. *TrAC Trends Analyt Chem* **2021**, *144*, 116424.

13. Magro, L.; Jacquelin, B.; Escadafal, C.; Garneret, P.; Kwasiborski, A.; Manuguerra, J.-C.; Monti, F.; Sakuntabhai, A.; Vanhomwegen, J.; Lafaye, P.; et al. Paper-based RNA detection and multiplexed analysis for Ebola virus diagnostics. *Sci. Rep.* **2017**, *7*, 1347.

14. Wang, Y.-C.; Tsai, Y.-H.; Shen, C.-F.; He, M.-Y.; Fu, Y.-C.; Sang, C.-Y.; Lee, Y.-T.; Cheng, C.-M. Turntable Paper-Based Device to Detect Escherichia coli. *Micromachines* **2021**, *12*.

15. Dong, M.; Sun, X.; Li, L.; He, K.; Wang, J.; Zhang, H.; Wang, L. A bacteria-triggered wearable colorimetric band-aid for real-time monitoring and treating of wound healing. *J. Colloid Interface Sci.* **2022**, *610*, 913-922.

16. Roy, S.; Bisaria, K.; Nagabooshanam, S.; Selvam, A.; Chakrabarti, S.; Wadhwa, S.; Singh, R.; Mathur, A.; Davis, J. An Electroanalytical Paper-Based Wound Dressing Using ZIF-67/C3 N4 Nanocomposite Towards the Monitoring of *Staphylococcus aureus* in Diabetic Foot Ulcer. *IEEE Sens. J.* **2021**, *21*, 1215-1221.

17. Ghaffari, R.; Rogers, J. A.; Ray, T. R. Recent progress, challenges, and opportunities for wearable biochemical sensors for sweat analysis. *Sens. Actuators B Chem.* **2021**, *332*, 129447.

18. Vaquer, A.; Barón, E.; de la Rica, R. Dissolvable Polymer Valves for Sweat Chrono-Sampling in Wearable Paper-Based Analytical Devices. *ACS Sens.* **2022**, *7*, 488-494.

19. Colozza, N.; Kehe, K.; Dionisi, G.; Popp, T.; Tsoutsoulopoulos, A.; Steinritz, D.; Moscone, D.; Arduini, F. A wearable origami-like paper-based electrochemical biosensor for sulfur mustard detection. *Biosens. Bioelectron.* **2019**, *129*, 15-23.

20. Li, S.; Ma, Z.; Cao, Z.; Pan, L.; Shi, Y. Advanced Wearable Microfluidic Sensors for Healthcare Monitoring. *Small* **2020**, *16*, 1903822.

21. Mogera, U.; Guo, H.; Namkoong, M.; Rahman, M. S.; Nguyen, T.; Tian, L. Wearable plasmonic paper–based microfluidics for continuous sweat analysis. *Sci. Adv.* **2022**, *8*, eabn1736.

22. Sempionatto, J. R.; Montiel, V. R.-V.; Vargas, E.; Teymourian, H.; Wang, J. Wearable and Mobile Sensors for Personalized Nutrition. *ACS Sens.* **2021**, *6*, 1745-1760.

23. Wu, Y.; Tehrani, F.; Teymourian, H.; Mack, J.; Shaver, A.; Reynoso, M.; Kavner, J.; Huang, N.; Furmidge, A.; Duvvuri, A.; et al. Microneedle Aptamer-Based Sensors for Continuous, Real-Time Therapeutic Drug Monitoring. *Anal. Chem.* **2022**, *94*, 8335-8345.

24. Tehrani, F.; Teymourian, H.; Wuerstle, B.; Kavner, J.; Patel, R.; Furmidge, A.; Aghavali, R.; Hosseini-Toudeshki, H.; Brown, C.; Zhang, F.; et al. An integrated wearable microneedle array for the continuous monitoring of multiple biomarkers in interstitial fluid. *Nat. Biomed. Eng.* **2022**.

25. Lin, Y.; Bariya, M.; Javey, A. Wearable Biosensors for Body Computing. *Adv. Funct. Mater.* **2021**, *31*, 2008087.

26. Mathew, M.; Radhakrishnan, S.; Vaidyanathan, A.; Chakraborty, B.; Rout, C. S. Flexible and wearable electrochemical biosensors based on two-dimensional materials: Recent developments. *Anal. Bioanal. Chem.* **2021**, *413*, 727-762.

27. Otero, F.; Magner, E. Biosensors—Recent Advances and Future Challenges in Electrode Materials. *Sensors* **2020**, *20*, 3561.

28. Liang, Y.; Luo, X.; Weng, W.; Hu, Z.; Zhang, Y.; Xu, W.; Bi, Z.; Zhu, M. Activated Carbon Nanotube Fiber Fabric as a High-Performance Flexible Electrode for Solid-State Supercapacitors. *ACS Appl. Mater. Interfaces* **2021**, *13*, 28433-28441.

29. Zhang, T.; Han, X.; Yang, H.; Han, A.; Hu, E.; Li, Y.; Yang, X.-q.; Wang, L.; Liu, J.; Liu, B. Atomically Dispersed Nickel(I) on an Alloy-Encapsulated Nitrogen-Doped Carbon Nanotube Array for High-Performance Electrochemical CO2 Reduction Reaction. *Angew. Chem. Int. Ed.* **2020**, *59*, 12055-12061.

30. Wang, M.; Yang, Y.; Min, J.; Song, Y.; Tu, J.; Mukasa, D.; Ye, C.; Xu, C.; Heflin, N.; McCune, J. S.; et al. A wearable electrochemical biosensor for the monitoring of metabolites and nutrients. *Nat. Biomed. Eng.* **2022**.

31. Ensafi, A. A.; Saberi, Z.; Kazemifard, N. 13 - Functionalized nanomaterial-based medical sensors for point-of-care applications: An overview. In *Functionalized Nanomaterial-Based Electrochemical Sensors*, Hussain, C. M., Manjunatha, J. G. Eds.; Woodhead Publishing, 2022; pp 277-308.

32. Kishnani, V.; Park, S.; Nakate, U. T.; Mondal, K.; Gupta, A. Nano-functionalized paper-based IoT enabled devices for point-of-care testing: a review. *Biomed. Microdevices* **2021**, *24*, 2.

33. Cho, I.-H.; Kim, D. H.; Park, S. Electrochemical biosensors: perspective on functional nanomaterials for on-site analysis. *Biomater. Res.* **2020**, *24*, 6.

34. Evans, E.; Moreira Gabriel, E. F.; Benavidez, T. E.; Tomazelli Coltro, W. K.; Garcia, C. D. Modification of microfluidic paper-based devices with silica nanoparticles. *Analyst* **2014**, *139*, 5560-5567.

35. Punjabi, K.; Adhikary, R. R.; Patnaik, A.; Bendale, P.; Saxena, S.; Banerjee, R. Lectin-Functionalized Chitosan Nanoparticle-Based Biosensor for Point-of-Care Detection of Bacterial Infections. *Bioconjugate Chem.* **2022**.

36. Nguyen, P. Q.; Soenksen, L. R.; Donghia, N. M.; Angenent-Mari, N. M.; de Puig, H.; Huang, A.; Lee, R.; Slomovic, S.; Galbersanini, T.; Lansberry, G.; et al. Wearable materials with embedded synthetic biology sensors for biomolecule detection. *Nat. Biotechnol.* **2021**, *39*, 1366-1374.

37. Sakar, M.; Chandan, H. R.; Shwetharani, R. Chapter 12 - Graphene Paper-Based Electrochemical Sensors for Biomolecules. In *Graphene-Based Electrochemical Sensors for Biomolecules*, Pandikumar, A., Rameshkumar, P. Eds.; Elsevier, 2019; pp 297-320.

38. Ray, T. R.; Choi, J.; Bandodkar, A. J.; Krishnan, S.; Gutruf, P.; Tian, L.; Ghaffari, R.; Rogers, J. A. Bio-Integrated Wearable Systems: A Comprehensive Review. *Chem. Rev.* **2019**, *119*, 5461-5533.

39. Duran, G. M.; Benavidez, T. E.; Giuliani, J. G.; Rios, A.; Garcia, C. D. Synthesis of CuNP-modified carbon electrodes obtained by pyrolysis of paper. *Sens. Actuators B Chem.* **2016**, *227*, 626-633.

40. Giuliani, J. G.; Benavidez, T. E.; Duran, G. M.; Vinogradova, E.; Rios, A.; Garcia, C. D. Development and characterization of carbon based electrodes from pyrolyzed paper for biosensing applications. *J. Electroanal. Chem.* **2016**, *765*, 8-15.

41. Ertl, P.; Robello, E.; Battaglini, F.; Mikkelsen, S. R. Rapid Antibiotic Susceptibility Testing via Electrochemical Measurement of Ferricyanide Reduction by Escherichia coli and Clostridium sporogenes. *Anal. Chem.* **2000**, *72*, 4957-4964.

42. Chotinantakul, K.; Suginta, W.; Schulte, A. Advanced Amperometric Respiration Assay for Antimicrobial Susceptibility Testing. *Anal. Chem.* **2014**, *86*, 10315-10322.

43. Catterall, K.; Robertson, D.; Hudson, S.; Teasdale, P. R.; Welsh, D. T.; John, R. A sensitive, rapid ferricyanide-mediated toxicity bioassay developed using Escherichia coli. *Talanta* **2010**, *82*, 751-757.

44. Ertl, P.; Wagner, M.; Corton, E.; Mikkelsen, S. R. Rapid identification of viable Escherichia coli subspecies with an electrochemical screen-printed biosensor array. *Biosens. Bioelectron.* **2003**, *18*, 907-916.

45. Suaifan, G. A. R. Y.; Alhogail, S.; Zourob, M. Rapid and low-cost biosensor for the detection of *Staphylococcus aureus*. *Biosens. Bioelectron.* **2017**, *90*, 230-237.

46. Sung, Y. J.; Suk, H.-J.; Sung, H. Y.; Li, T.; Poo, H.; Kim, M.-G. Novel antibody/gold nanoparticle/magnetic nanoparticle nanocomposites for immunomagnetic separation and rapid colorimetric detection of *Staphylococcus aureus* in milk. *Biosens. Bioelectron.* **2013**, *43*, 432-439.

47. Asif, M.; Awan, F. R.; Khan, Q. M.; Ngamsom, B.; Pamme, N. Paper-based analytical devices for colorimetric detection of S. aureus and E. coli and their antibiotic resistant strains in milk. *Analyst* **2020**, *145*, 7320-7329.

48. Bekir, K.; Barhoumi, H.; Braiek, M.; Chrouda, A.; Zine, N.; Abid, N.; Maaref, A.; Bakhrouf, A.; Ouada, H. B.; Jaffrezic-Renault, N.; et al. Electrochemical impedance immunosensor for rapid detection of stressed pathogenic *Staphylococcus aureus* bacteria. *Environ Sci Pollut Res* **2015**, *22*, 15796-15803.

49. Eissa, S.; Zourob, M. A dual electrochemical/colorimetric magnetic nanoparticle/peptide-based platform for the detection of Staphylococcus aureus. *Analyst* **2020**, *145*, 4606-4614.

50. Primiceri, E.; Chiriacò, M. S.; de Feo, F.; Santovito, E.; Fusco, V.; Maruccio, G. A multipurpose biochip for food pathogen detection. *Anal. Methods* **2016**, *8*, 3055-3060.

51. Dominguez, T. J. It's Not a Spider Bite, It's Community-Acquired Methicillin-Resistant *Staphylococcus aureus*. *J Am Board Fam Med* **2004**, *17*, 220.

52. Börjesson, S.; Gómez-Sanz, E.; Ekström, K.; Torres, C.; Grönlund, U. *Staphylococcus* pseudintermedius can be misdiagnosed as *Staphylococcus aureus* in humans with dog bite wounds. *Eur. J. Clin. Microbiol. Infect. Dis.* **2015**, *34*, 839-844.

53. Karakonstantis, S. Is coverage of S. aureus necessary in cellulitis/erysipelas? A literature review. *Infection* **2020**, *48*, 183-191.

54. Cesewski, E.; Johnson, B. N. Electrochemical biosensors for pathogen detection. *Biosens. Bioelectron.* **2020**, *159*, 112214.

55. Riu, J.; Giussani, B. Electrochemical biosensors for the detection of pathogenic bacteria in food. *TrAC Trends Analyt Chem* **2020**, *126*, 115863.

56. Pujol-Vila, F.; Vigués, N.; Guerrero-Navarro, A.; Jiménez, S.; Gómez, D.; Fernández, M.; Bori, J.; Vallès, B.; Riva, M. C.; Muñoz-Berbel, X.; et al. Paper-based chromatic toxicity bioassay by analysis of bacterial ferricyanide reduction. *Anal. Chim. Acta* **2016**, *910*, 60-67.

57. Rao R, P.; Sharma, S.; Mehrotra, T.; Das, R.; Kumar, R.; Singh, R.; Roy, I.; Basu, T. Rapid Electrochemical Monitoring of Bacterial Respiration for Gram-Positive and Gram-Negative Microbes: Potential Application in Antimicrobial Susceptibility Testing. *Anal. Chem.* **2020**, *92*, 4266-4274.

58. Davis, J. A.; Farrah, S. R.; Wilkie, A. C. Selective growth of *Staphylococcus aureus* from flushed dairy manure wastewater using acriflavine-supplemented mannitol salt agar. *Lett. Appl. Microbiol.* **2006**, *42*, 606-611.

59. Lagler, H.; Bangert, C.; Quint, T.; Österreicher, Z.; Nussbaumer-Pröll, A.; Eberl, S.; Weber, M.; Karer, M.; Sommer, M. O. A.; Zeitlinger, M. Comparison of non-invasive *Staphylococcus aureus* sampling methods on lesional skin in patients with atopic dermatitis. *Eur. J. Clin. Microbiol.* **2022**, *41*, 245-252.

60. Silva, L. A. J.; da Silva, W. P.; Giuliani, J. G.; Canobre, S. C.; Garcia, C. D.; Munoz, R. A. A.; Richter, E. M. Use of pyrolyzed paper as disposable substrates for voltammetric determination of trace metals. *Talanta* **2017**, *165*, 33-38.

61. Santos, M. S. F.; Ameku, W. A.; Gutz, I. G. R.; Paixão, T. R. L. C. Gold leaf: From gilding to the fabrication of disposable, wearable and low-cost electrodes. *Talanta* **2018**, *179*, 507-511.

62. Prasertying, P.; Jantawong, N.; Sonsa-ard, T.; Wongpakdee, T.; Khoonrueng, N.; Buking, S.; Nacapricha, D. Gold leaf electrochemical sensors: applications and nanostructure modification. *Analyst* **2021**, *146*, 1579-1589.

63. Zamani, M.; Robson, J. M.; Fan, A.; Bono, M. S.; Furst, A. L.; Klapperich, C. M. Electrochemical Strategy for Low-Cost Viral Detection. *ACS Cent. Sci.* **2021**, *7*, 963-972.

64. Hong, S. H.; Kraiya, C.; Lehmann, M. W.; Evans, D. H. Evaluation of Uncompensated Solution Resistance for Electrodes with Spherical-Cap Geometry. *Anal. Chem.* **2000**, *72*, 454-458.

65. Navarro-Laboulais, J.; Trijueque, J.; Vicente, F.; Scholl, H. Voltammetric determination of optimal conductive load proportion in graphite—epoxy composite electrodes. *J. Electroanal. Chem.* **1994**, *379*, 159-163.

66. Valentini, F.; Amine, A.; Orlanducci, S.; Terranova, M. L.; Palleschi, G. Carbon Nanotube Purification: Preparation and Characterization of Carbon Nanotube Paste Electrodes. *Anal. Chem.* **2003**, *75*, 5413-5421.

67. Adkins, J. A.; Henry, C. S. Electrochemical detection in paper-based analytical devices using microwire electrodes. *Anal. Chim. Acta* **2015**, *891*, 247-254.

68. Gomez, F. J. V.; Chumanov, G.; Silva, M. F.; Garcia, C. D. CO2 reduction using paper-derived carbon electrodes modified with copper nanoparticles. *RSC Adv.* **2019**, *9*, 33657-33663.

69. Buaki-Sogó, M.; García-Carmona, L.; Gil-Agustí, M.; García-Pellicer, M.; Quijano-López, A. Flexible and Conductive Bioelectrodes Based on Chitosan-Carbon Black Membranes: Towards the Development of Wearable Bioelectrodes. *Nanomaterials* **2021**, *11*.

70. Zheng, H.; Chen, G.; Gan, L.; Liu, J.; Lin, L. Iron-Adjustable Compressible Elastic Chitosan-Derived Carbon Aerogel with Wide-Range Linear Sensitivity and Super Sensing Performances for Wearable Piezoresistive Sensors. *ACS Sustain. Chem. Eng.* **2022**, *10*, 10604-10614.

71. Elgrishi, N.; Rountree, K. J.; McCarthy, B. D.; Rountree, E. S.; Eisenhart, T. T.; Dempsey, J. L. A Practical Beginner's Guide to Cyclic Voltammetry. *J. Chem. Ed.* **2018**, *95*, 197-206.

72. Nicoliche, C. Y. N.; Pascon, A. M.; Bezerra, Í. R. S.; de Castro, A. C. H.; Martos, G. R.; Bettini, J.; Alves, W. A.; Santhiago, M.; Lima, R. S. In Situ Nanocoating on Porous Pyrolyzed Paper Enables Antibiofouling and Sensitive Electrochemical Analyses in Biological Fluids. *ACS Appl. Mater. Interfaces* **2022**, *14*, 2522-2533.

73. Shimizu, F. M.; Pasqualeti, A. M.; Nicoliche, C. Y. N.; Gobbi, A. L.; Santhiago, M.; Lima, R. S. Alcohol-Triggered Capillarity through Porous Pyrolyzed Paper-Based Electrodes Enables Ultrasensitive Electrochemical Detection of Phosphate. *ACS Sens.* **2021**, *6*, 3125-3132.

74. Zang, D.; Ge, L.; Yan, M.; Song, X.; Yu, J. Electrochemical immunoassay on a 3D microfluidic paper-based device. *Chem. Comm.* **2012**, *48*, 4683-4685.

75. Ibrahim, H. M.; Zairy, E. M. R. E. Chitosan as a Biomaterial@ Structure, Properties, and Electrospun Nanofibers. 2015.

76. Qiu, J.-D.; Wang, R.; Liang, R.-P.; Xia, X.-H. Electrochemically deposited nanocomposite film of CS-Fc/Au NPs/GOx for glucose biosensor application. *Biosens. Bioelectron.* **2009**, *24*, 2920-2925.

77. Hohendorff, B.; Weidermann, C.; Burkhart, K. J.; Rommens, P. M.; Prommersberger, K. J.; Konerding, M. A. Lengths, girths, and diameters of children's fingers from 3 to 10 years of age. *Ann. Anat.* **2010**, *192*, 156-161.

78. Meloni, G. N. Building a Microcontroller Based Potentiostat: A Inexpensive and Versatile Platform for Teaching Electrochemistry and Instrumentation. *J. Chem. Ed.* **2016**, *93*, 1320-1322.

79. Rowe, A. A.; Bonham, A. J.; White, R. J.; Zimmer, M. P.; Yadgar, R. J.; Hobza, T. M.; Honea, J. W.; Ben-Yaacov, I.; Plaxco, K. W. CheapStat: An Open-Source, “Do-It-Yourself” Potentiostat for Analytical and Educational Applications. *PLOS One* **2011**, *6*, e23783.

80. Cordova-Huaman, A. V.; Jauja-Ccana, V. R.; La Rosa-Toro, A. Low-cost smartphone-controlled potentiostat based on Arduino for teaching electrochemistry fundamentals and applications. *Heliyon* **2021**, *7*, e06259.

81. Pereira de Oliveira, L.; Rocha, D. P.; Reis de Araujo, W.; Abarza Muñoz, R. A.; Longo Cesar Paixão, T. R.; Oliveira Salles, M. Forensics in hand: new trends in forensic devices (2013–2017). *Anal. Methods* **2018**, *10*, 5135-5163.

82. Noviana, E.; Carrão, D. B.; Pratiwi, R.; Henry, C. S. Emerging applications of paper-based analytical devices for drug analysis: A review. *Anal. Chim. Acta* **2020**, *1116*, 70-90.

83. Edwards, K. G.; Blumenthal, H. J.; Khan, M.; Slodki, M. E. Intracellular mannitol, a product of glucose metabolism in staphylococci. *J Bacteriol* **1981**, *146*, 1020-1029.

84. Murphey, W. H.; Rosenblum, E. D. Mannitol Catabolism By *Staphylococcus aureus*. *Arch Biochem Biophys* **1964**, *107*, 292-297.

85. Nguyen, T.; Kim, T.; Ta, H. M.; Yeo, W. S.; Choi, J.; Mizar, P.; Lee, S. S.; Bae, T.; Chaurasia, A. K.; Kim, K. K. Targeting Mannitol Metabolism as an Alternative Antimicrobial Strategy Based on the Structure-Function Study of Mannitol-1-Phosphate Dehydrogenase in *Staphylococcus aureus*. *mBio* **2019**, *10*.

86. Rubab, M.; Shahbaz, H. M.; Olaimat, A. N.; Oh, D.-H. Biosensors for rapid and sensitive detection of Staphylococcus aureus in food. *Biosens. Bioelectron.* **2018**, *105*, 49-57.

87. Simoska, O.; Stevenson, K. J. Electrochemical sensors for rapid diagnosis of pathogens in real time. *Analyst* **2019**, *144*, 6461-6478.

88. Gill, A. A. S.; Singh, S.; Thapliyal, N.; Karpoormath, R. Nanomaterial-based optical and electrochemical techniques for detection of methicillin-resistant Staphylococcus aureus: a review. *Microchim. Acta* **2019**, *186*, 114.

89. Samani, S. S.; Khojastehnezhad, A.; Ramezani, M.; Alibolandi, M.; Yazdi, F. T.; Mortazavi, S. A.; Khoshbin, Z.; Abnous, K.; Taghdisi, S. M. Ultrasensitive detection of micrococcal nuclease activity and Staphylococcus aureus contamination using optical biosensor technology-A review. *Talanta* **2021**, *226*, 122168.

90. Cui, F.; Sun, J.; de Dieu Habimana, J.; Yang, X.; Ji, J.; Zhang, Y.; Lei, H.; Li, Z.; Zheng, J.; Fan, M.; et al. Ultrasensitive Fluorometric Angling Determination of Staphylococcus aureus in Vitro and Fluorescence Imaging in Vivo Using Carbon Dots with Full-Color Emission. *Anal. Chem.* **2019**, *91*, 14681-14690.

91. Cai, R.; Zhang, Z.; Chen, H.; Tian, Y.; Zhou, N. A versatile signal-on electrochemical biosensor for Staphylococcus aureus based on triple-helix molecular switch. *Sens. Actuators B Chem.* **2021**, *326*, 128842.

92. Zhu, A.; Jiao, T.; Ali, S.; Xu, Y.; Ouyang, Q.; Chen, Q. SERS Sensors Based on Aptamer-Gated Mesoporous Silica Nanoparticles for Quantitative Detection of Staphylococcus aureus with Signal Molecular Release. *Anal. Chem.* **2021**, *93*, 9788-9796.

93. Chen, L.; Leng, Y.-K.; Liu, B.; Liu, J.; Wan, S.-P.; Wu, T.; Yuan, J.; Shao, L.; Gu, G.; Fu, Y. Q.; et al. Ultrahigh-sensitivity label-free optical fiber biosensor based on a tapered singlemode- no core-singlemode coupler for Staphylococcus aureus detection. *Sens. Actuators B Chem.* **2020**, *320*, 128283.

94. Xue, J.-W.; Wang, R.; Yang, J.-Y.; Wang, L.-X.; Cao, Y.; Li, H.-D.; Yang, T.; Wang, J.-H. Sensitive plasmonic ELISA assay based on butyrylcholinesterase catalyzed hydrolysis for the detection of Staphylococcus aureus. *Sens. Actuators B Chem.* **2022**, *365*, 131948.

95. Chen, J.; Sun, Y.; Peng, X.; Ni, Y.; Wang, F.; Dou, X. Rapid Analysis for Staphylococcus aureus via Microchip Capillary Electrophoresis. In *Sensors*, 2021; Vol. 21.

96. Pardo-Castaño, C.; Bolaños, G. Solubility of chitosan in aqueous acetic acid and pressurized carbon dioxide-water: Experimental equilibrium and solubilization kinetics. *J Supercrit Fluids* **2019**, *151*, 63-74.

Supplementary Information for

Rapid Detection of *Staphylococcus aureus* Using Paper-Derived Electrochemical Biosensors

Lucas de Brito Ayres, Jordan Brooks, Kristi Whitehead, and Carlos D. Garcia

Table of contents

1. ADDITIONAL EXPERIMENTAL DETAILS

1.1. Solutions and Reagents. All solutions were prepared using Milli-Q Water (18 MΩ.cm, Direct-Q, Millipore Sigma, Burlington, MA, USA) and analytical-grade reagents. Phosphate-buffered saline (PBS, at 0.01M and pH 7.4) was used as supporting electrolyte and prepared by dissolving sodium chloride (J.T Baker, Phillipsburg, NJ, USA), potassium chloride (EM Science, Gibbstown, NJ, USA), sodium phosphate dibasic (Fisher Chemical, Fair Lawn, NJ, USA) and potassium phosphate monobasic (Sigma-Aldrich, St. Louis MO, USA). Potassium ferrocyanide trihydrate was purchased from Fischer Scientific (Fischer Chemical, NJ, USA), D-mannitol and potassium ferricyanide (III) were purchased from (Sigma-Aldrich, St. Louis MO, USA). The pH of the solution was measured using a glass electrode connected to a digital pH meter (Orion 420A +, Thermo; Waltham, MA, USA) and adjusted with a 1 $mol \cdot L^{-1}$ solution of either NaOH or HCl.

1.2. Chitosan preparation. The solution of the polymer was prepared by dissolving medium-molecular weight chitosan (Sigma-Aldrich, Milwaukee, Burlington, WI, USA) in 2% acetic acid solutions (Fischer Chemical, NJ, USA) with gentle stirring overnight. The resulting biopolymers, at concentrations of either 0.5%, 1.0%, 1.5% or 2.0%, were stored in the fridge in sealed falcon tubes until use. It is important to mention that while it is possible to prepare solutions containing higher concentrations of the polymer,[86] they were considered outside the experimental design due their preparation conditions and resulting viscosity.

1.3. Electrochemical experiments. Cyclic voltammetry (CV) was initially performed to investigate the electrochemical performance of the proposed electrodes. The experiments were performed using 0.01 M PBS containing 1 mM $K_3Fe(CN)_6$ / $K_4Fe(CN)_6$ as the redox couple and carried out using either a CHI660A Electrochemical Analyzer (CH Instruments, Inc.; Austin, TX) or the proposed potentiostat. Electrochemical impedance spectroscopy (EIS) experiments were performed under the same experimental conditions, by scanning from 10^{-4} Hz to 10^{5} Hz at a 5 mV amplitude, with 10 data points per frequency decade. The impedance spectra were then analyzed with the simulation software Zview-Impedance® (version 2.4a) by fitting the spectra with a Randles-type equivalent circuit.

1.4. *S. aureus* and *E. coli* preparation. *S. aureus* (ATCC 25923) and *E. coli* (ATCC) were both recovered from freezer stocks by streaking onto Mueller Hinton II plates. The plates were then incubated aerobically at 37 °C for 24 hours. A liquid culture was grown by inoculating a single colony from each plate into 10mL of Tryptic-Soy Broth and incubating aerobically at 37 °C for 24 hours. 100uL of each liquid culture was then spread-plated onto Muller Hinton II phases. The spread plates were incubated aerobically at 37 °C for 24 hours prior to electrochemical analysis. Detection experiments involving bacteria were performed in a laminar-flow hood (disinfected prior and after use) and at room temperature.

1.5 Electronic Circuits and components. The circuit's layout was developed using the Altium Designer 21.4.1 software and it is schematically shown in Figure SI 1. The dual layer printed circuit board was made inn Fr-4 material and was manufactured by NextPCB (Shenzhen, China). ESP 32 (Devkit v1) was used as microcontroller of the instrument and provides of a low energy Wi-Fi and Bluetooth built in-chip, 12 bits analogic to digital converter (ADC) as well as 8 bits digital to analogic converter (DAC). The LM324 Quad-Operational Amplifier was used as frequency filter, voltage adder, transimpedance amplifier as well as voltage fallower. The electronic component ICL 7660A was used as positive to negative voltage converter aiming to symmetrically power supply the operational amplifiers. Additionally, a 5000mAh / 5V portable phone charger (Alongza, with Li-ion battery, 1A and 2.1 dual USB output) was used as a rechargeable battery for the instrument developed.

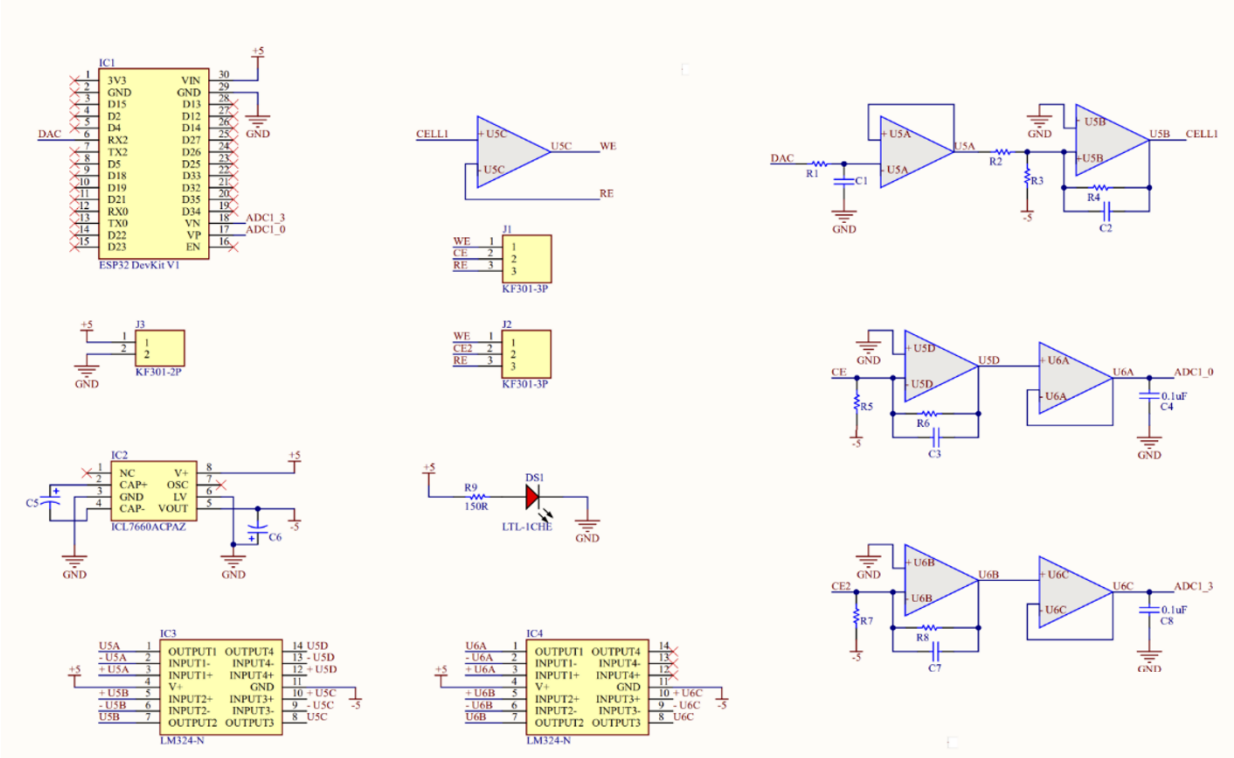

Figure SI 1: Electronic diagram of the proposed portable potentiostat.

General User Interface (GUI) and back end. Node JavaScript was used to develop the GUI for web browsers. In the server side, Paho JavaScript Client was used as external library to connect the GUI to the Eclipse Broker using a WebSocket technology. The software is responsible to assign the GUI to the Internet of Things (IoT) MQTT Broker, to send instructions in a string format to the portable potentiostat as well as receive data from electrochemical analysis (CV or amperometry).

Firmware. The main firmware implemented in the microcontroller was programmed in Arduino IDE, a program language similar to C++. The firmware is responsible to assign the portable instrument to the IOT MQTT broker, receive instructions from the user as well as consign data acquired from electrochemical analysis.

2. ELECTROCHEMICAL CHARACTERIZATION

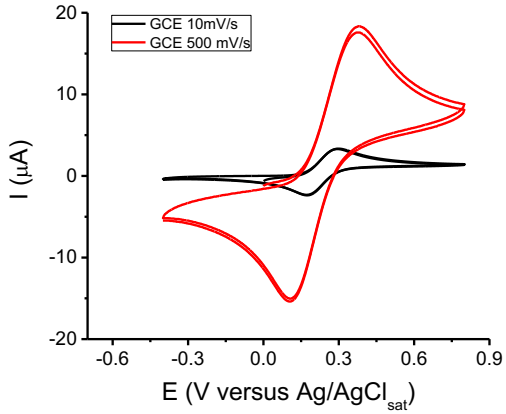

Figure SI 2A: I vs E profiles obtained as a function of the scan rate with a glassy carbon electrode (GCE). Conditions: 5mM ferrocyanide in 0.01 PBS buffer, pH 7.4.

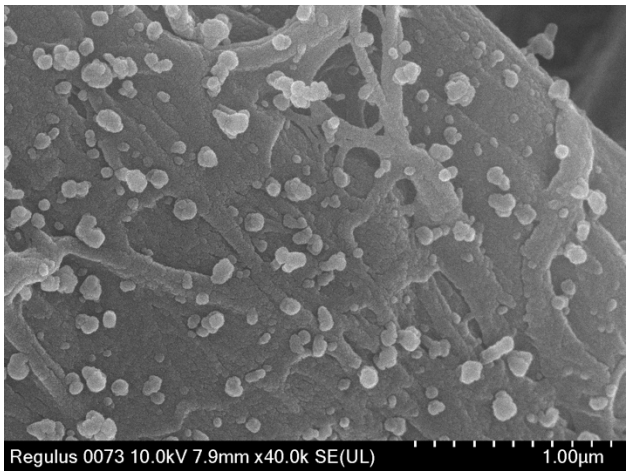

Figure SI 2B: SEM image of the pyrolyzed cellulose after sputtering the gold layer (35 µg/cm^2) on the surface

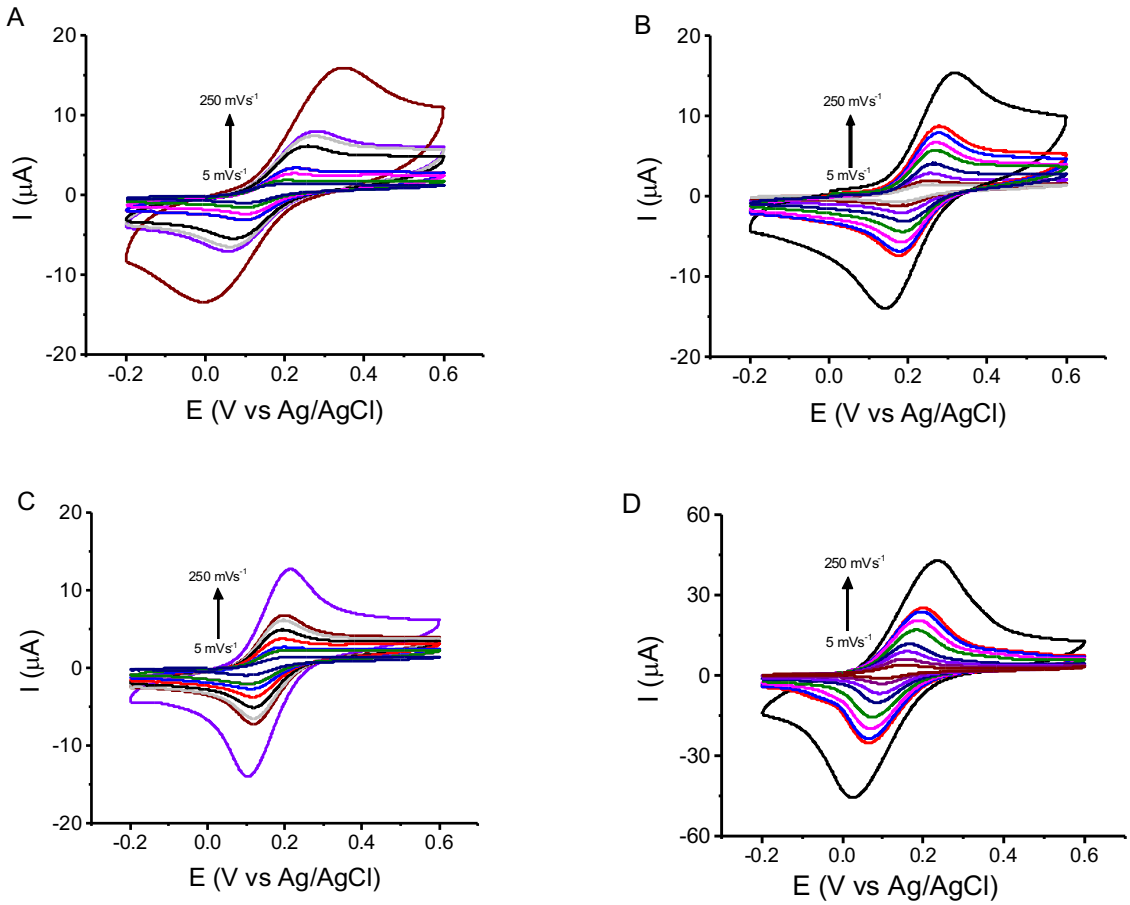

Figure SI 3: I vs E profiles obtained as a function of the scan rate with the paper-derived sensors modified with gold and chitosan at 0% (A, control), 0.5% (B), 1.0% (C), or 2.0% (D). Conditions: 5mM ferrocyanide in 0.01 PBS buffer, pH 7.4.

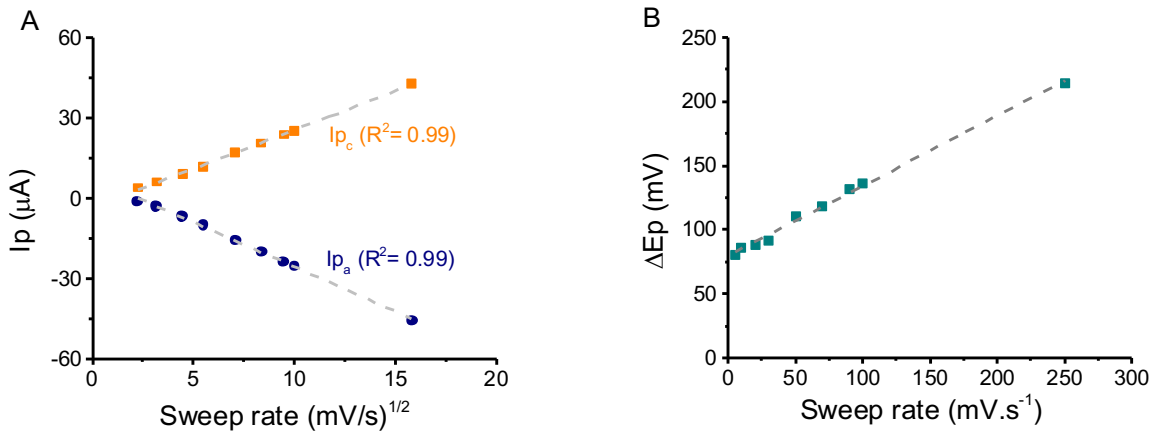

Figure SI 4: Relation of the peak current (Ip) as a function the square root of the sweep rate (A) and peak potential difference (ΔEp) as a function of the sweep rate (B) for the proposed paper-derived electrodes modified with 2.0% chitosan. Conditions: 5mM ferri/ferrocyanide in PBS at several sweep rates and in the -0.2V to +0.6V range.

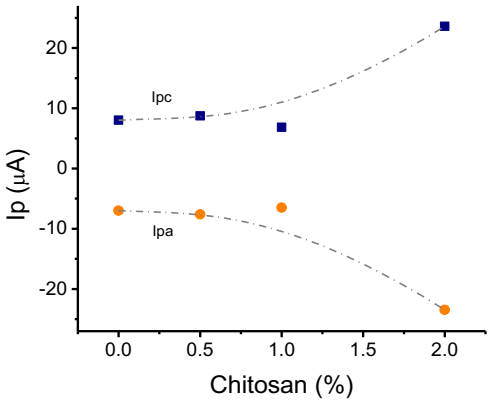

Figure SI 5: Dependence of the peak current (obtained at 100 mV.s^{-1}) as a function of the concentration of chitosan, calculated from the voltammograms in Figure SI 3.

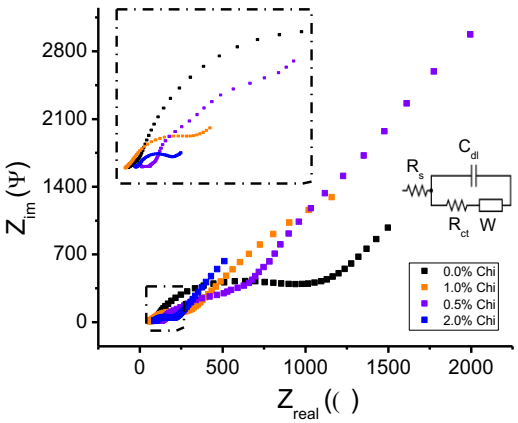

Figure SI 6: Effect of the concentration of chitosan used to modify the electrode on the electrochemical response, obtained via electrochemical impedance spectroscopy. Conditions: 5mM ferrocyanide in 0.01M PBS buffer at a half-wave potential of 0.15V.

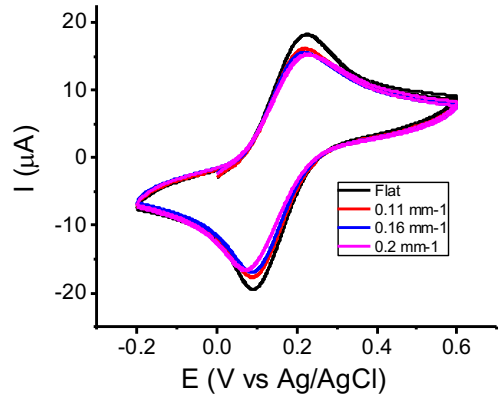

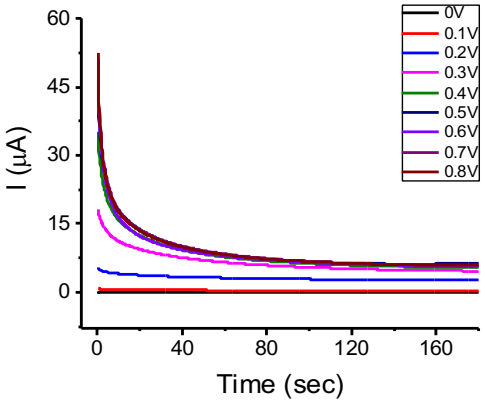

Figure SI 7: Effect of the electrode curvature on the electrochemical response for the proposed paper-derived electrodes modified with 2.0% chitosan. Conditions: 5mM ferri/ferrocyanide in PBS, pH 7.4, sweep rate: 50mV.s^{-1}.

Figure SI 8: Amperometric curve registred in funcion of time at 0, 0.1V, 0.2V, 0.3V, 0.4V, 0.5V, 0.6V, 0.7V, and 0.8V. Conditions: 5mM ferri/ferrocyanide in PBS, pH 7.4.

3. ELECTRONICS AND INSTRUMENTATION VALIDATION

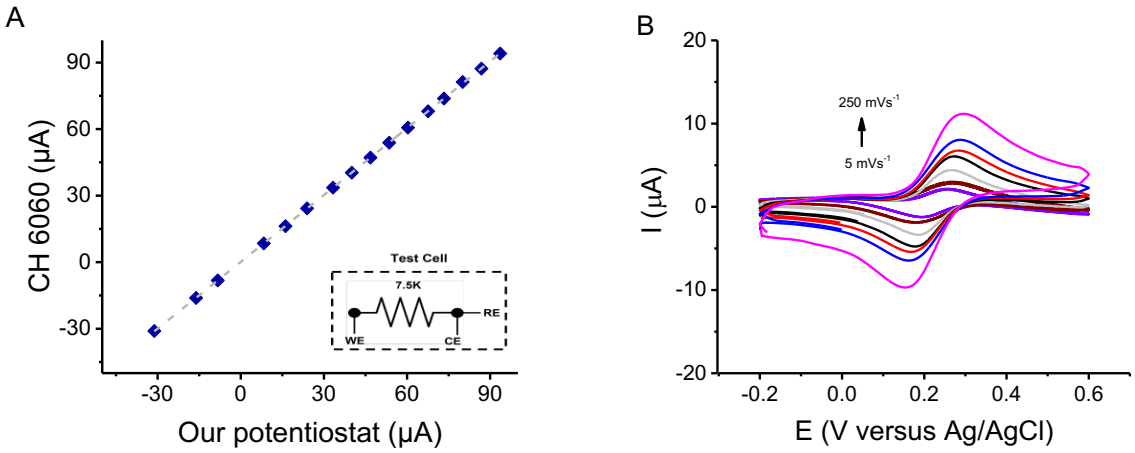

Figure SI 9: Polizarion curve registred by using the proposed portable potentiostat and the comercial instrument (A). Cyclic voltmmogram registred by the portable potentiostat at several sweep rates (B). Conditions: 5mM ferri/ferrocyanide in PBS (pH 7.4).

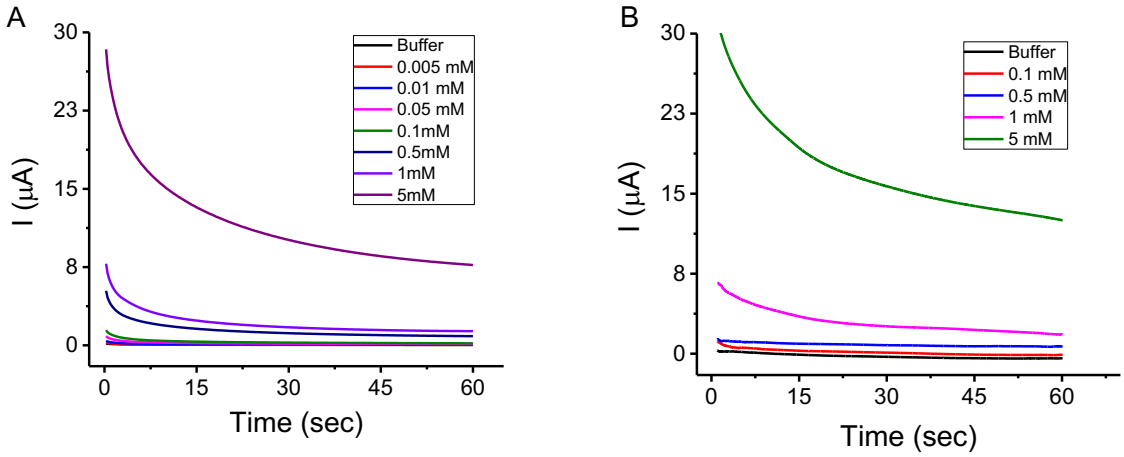

Figure SI 10: Amperometric curve registred in funcion of time by the comercial instrument (A) and the proposed portable potentiotsat (B). Conditions: Ferri/ferrocyanide at several concentratiosn in PBS pH 7.4, applied potential 0.4V.

4. DETECTION OF BACTERIA

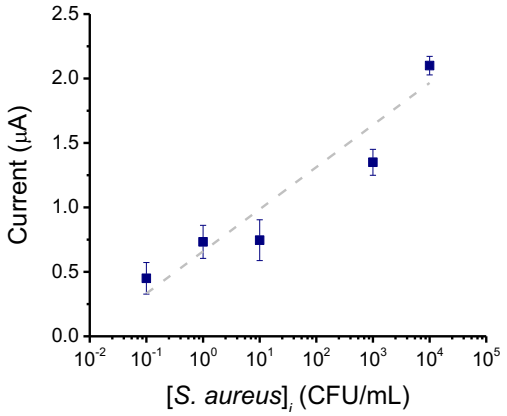

Figure SI 11: Current developed as a function of the initial concentration of bacterial *S. aureus* after 60 min incubation. Conditions: 2.5 mM $K_4Fe[CN]_6$ diluted in PBS, detection potential: +0.4V, each measured at 45 sec. Line included to guide the eye.